Talanta 97 (2012) 368–375

Contents lists available at SciVerse ScienceDirect

Talanta

journal homepage: www.elsevier.com/locate/talanta

A SERS and fluorescence dual mode cancer cell targeting probe based on silica coated Au@Ag core–shell nanorods

Shenfei Zong, Zhuyuan Wang, Jing Yang, Chunlei Wang, Shuhong Xu, Yiping Cui *

Advanced Photonics Center, Southeast University, Nanjing 210096, Jiangsu, China

ARTICLE INFO

Article history:
Received 18 February 2012
Received in revised form
12 April 2012
Accepted 21 April 2012
Available online 30 April 2012

Keywords:
Surface enhanced Raman scattering
Fluorescence
Dual mode
Cancer cell targeting
Quantum dots
Au@Ag core–shell nanorods

ABSTRACT

We report a dual mode cancer cell targeting probe based on CdTe quantum dots (QDs) conjugated, silica coated Au@Ag core–shell nanorods (Au@Ag NRs), which can generate both surface enhanced Raman scattering (SERS) and fluorescence signals. In such a probe, folic acid (FA) is used as a targeting ligand for folate receptors (FRs) overexpressed cancer cells. To synthesize the probe, Au@Ag NRs were first prepared to serve as the SERS substrates by coating an Ag shell on the gold nanorods. Then the Au@Ag NRs were labeled with 4-mercaptobenzoic acid (4MBA) to generate SERS signals, followed by being coated with a silica shell through a modified Stöber method. Finally, CdTe QDs and FA were conjugated to the silica coated Au@Ag NRs by the carbodiimide chemistry to yield fluorescence and the targeting ability, respectively. To validate the targeting capability of the probe, *in vitro* experiments were conducted, using HeLa cells with overexpressed FRs as the model target cells and MRC-5 cells with a low folate receptor expression level as the negative control. Both the fluorescence imaging and the SERS mapping results confirmed that the proposed probe can be used as an efficient cancer cell targeting agent. This kind of multifunctional probe has great potential in the diagnosis and therapeutics of cancerous diseases due to its specific targeting and multiplex imaging abilities, especially in the simultaneous tracking of multiple components in a hybrid bio-system.

1. Introduction

Today, selective targeting and imaging of malignant cells are becoming more and more crucial for the diagnosis and treatment of the cancerous diseases [1]. Functionalized nanoprobes based mesoporous silica [2], metal nanoparticles [3] and carbon nanotubes [4], have attracted massive attention concerned with their design and fabrication. The selective targeting of these nanoprobes to the cancer cells is realized by modifying their surfaces with specific antibodies or ligands [5–8]. Folic acid (FA) has emerged as a popular ligand for the cancer cell targeting, because folate receptors (FRs) are often overexpressed on the membranes of many kinds of human cancer cells [9]. As a result, FA conjugated nanoprobes are capable of distinguishing the cancer cells from the healthy ones and triggering the specific cancer cell uptake via the FRs mediated endocytosis [2,10,11].

In the design of a targeting probe, it is desirable that the abilities to target the specific cancer cells and generate observable optical signals are combined together into one single targeting system, making it possible to directly track and monitor the targeting events. In the past years, fluorescence based imaging technique is widely employed in the investigation of the cancer cell targeting [12,13]. A vast variety of materials, such as organic fluorophores [14], upconverting nanoparticles [15] and semiconductor nanocrystals (quantum dots) [16,17], have been employed as the contrast agents for the fluorescence imaging. Among these, quantum dots (QDs) species have been considered as a promising luminescent candidate [18,19], because of their tunable fluorescence emission properties with a high quantum yield and photostability.

Recently, Raman scattering enhanced by novel metal nanoparticles (NPs) has opened up a new avenue towards the field of bioimaging and biosensing [20–23]. Since its discovery, surface enhanced Raman scattering (SERS) has been used as a molecular and cellular analytical technology with an extremely high sensitivity [24–26]. The intriguing potential bio-applications of SERS have boosted the design and fabrication of new efficient SERS substrates, such as nanocages [27], nanorods [28,29], alloy nanoshells [30], hollow nanospheres [31] and so on, which are mainly composed of silver and gold. An interesting approach to prepare silver NPs with well tailored morphology is to use the preformed gold NPs as the templates for silver coating [32–36]. It has been reported that the Au@Ag core–shell nanorods (Au@Ag NRs) with a good shape and size monodispersity can be obtained by coating the gold nanorods (GNRs) with a layer of silver [32,34,36].

However, both of the fluorescence and SERS based techniques exhibit some intrinsic disadvantages. For example, the spectral

* Corresponding author. Tel.: 86 25 83601769x828; fax: 86 25 83601769x838.
E-mail address: cyp@seu.edu.cn (Y. Cui).

0039-9140/$ - see front matter © 2012 Elsevier B.V. All rights reserved.
http://dx.doi.org/10.1016/j.talanta.2012.04.047

overlap of fluorescence restricts its further applications in multiplexed bioimaging and biosensing. Meanwhile, compared with fluorescence, SERS requires a relatively long acquisiton time due to its weak intensity, which hinders its applications in high-speed and real-time analysis. As a result, the combination of the two techniques could be an attractive solution. Recently, a new strategy which integrates the fluorescence and SERS signals into a single composite nanoparticle has emerged, using organic dyes as the fluorescence generators and gold NPs as the SERS substrates [8,37–39]. However, the sensitivity and multiplexing capability of such nanocomposite particles are limited by the generally wide emission bands of the organic dyes.

Herein, we demonstrate the synthesis of a SERS and fluorescence dual mode imaging probe with the capability of targeting cancer cells. The proposed probe consists of three main functional components, including CdTe QDs served as the contrast agents for fluorescence imaging, 4-mercaptobenzoic acid (4MBA) labeled Au@Ag NRs served as the generator of SERS signals for SERS mapping, and FA served as the targeting ligand. In such a designed structure, QDs have much narrower emission spectra than the organic dyes while the Au@Ag NRs can provide a much stronger SERS enhancement than gold NPs. Using human cervical cancer cells (HeLa cells) with overexpressed FRs as the model target cells, the cancer cell targeting ability of the proposed probe was examined. Experimental results revealed that the biorecognition towards specific cancer cell lines can be fulfilled by the presented targeting probe. This kind of multifunctional probe with prospective multiplexing capability has great potential in the tracking and verification of the biological procedures in living cells, such as the interaction between the NPs and cells in the specific recognition or targeted drug delivery systems.

2. Experimental section

2.1. Materials

Hydrogen tetrachloroaurate(III) trihydrate ($HAuCl_4 \cdot 3H_2O$), silver nitrate ($AgNO_3$), sodium borohydride ($NaBH_4$), poly(vinylpyrrolidone) (PVP, MW 8000), poly(ethyleneimine) (PEI, MW 10,000), tetraethoxysilane (TEOS), cetyltrimethylammonium bromide (CTAB) and absolute ethanol were purchased from Alfa Aesar. Poly (allylamine hydrochloride) (PAH, MW 15,000), 4-mercaptobenzoic acid (4MBA), 1-ethyl-3-(3-dimethylaminopropyl) carbodiimide (EDC) and N-hydroxysuccinimide (NHS) were purchased from Sigma Aldrich. Folic acid (FA) was purchased from Aladdin Reagent Co., Ltd. Ascorbic acid (AA) was purchased from Shanghai Shisihewei Chemical Co., Ltd. Ammonia water was purchased from Shanghai Zhongshi Chemical Co., Ltd. Sodium hydroxide (NaOH) and sodium chloride (NaCl) were purchased from Guangdong Xilong Chemical Co., Ltd. Phosphate buffered saline (PBS, pH 7.4) was purchased from Nanjing Bookman Biotechnology Co., Ltd. All the reagents were used as received. Deionized water (Millipore Milli-Q grade) with resistivity of 18.2 MΩ cm^{-1} was used in all the experiments.

2.2. Synthesis of the cancer cell targeting probe

The synthesis procedure of the targeting probe, which is well established and quite reproducible, is illustrated in Scheme 1. In the structure of such a probe, the 4MBA labeled Au@Ag NRs are encapsulated by a silica shell while the CdTe QDs and FA are covalently linked to the surface of the silica shell.

2.2.1. Synthesis of the Au@Ag core–shell nanorods (denoted as Au@Ag NRs)

The Au@Ag NRs were synthesized according to a previously published literature, using GNRs as the seeds [36]. GNRs were prepared by the seed-mediated growth method [40]. To remove excess reagents, 24 mL of the as-prepared GNRs solution was centrifuged twice at 10,000 rpm for 30 min. The precipitate was dispersed in 12 mL of deionized water. This purified GNRs solution was then added to 60 mL of 0.04 M CTAB aqueous solution under vigorous stirring with the temperature being kept at 30 °C. Then 1.56 mL of 0.1 M AA, 2.5 mL of 10 mM $AgNO_3$ and 3.48 mL of 0.1 M NaOH solution were added sequentially. The color of the solution changed rapidly from brown to rose, indicating the formation of the Au@Ag NRs.

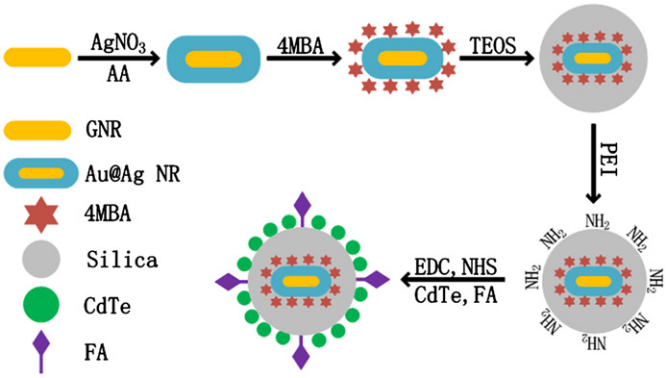

Scheme 1. The synthesis procedure of the cancer cell targeting probe.

2.2.2. Adsorption of the Raman reporter molecules onto Au@Ag NRs

Raman reporter molecules (4MBA) were adsorbed onto the surfaces of the Au@Ag NRs to make these NPs SERS active. First, 5 mL of the as-prepared Au@Ag NRs solution was centrifuged at 10,000 rpm for 30 min to remove the excess reagents. The precipitate was dispersed in 5 mL of deionized water. Then 5 μL of 10 mM 4MBA ethanol solution was added and agitated for 3 h at 45 °C. Unbonded 4MBA molecules were removed by centrifugation once at 8000 rpm for 30 min. After discarding the supernatant, the precipitate was suspended in 5 mL of 2 mg/mL PAH (in 2 mM NaCl) solution and gently stirred for 1 h. Excess PAH was removed by centrifugation once at 8000 rpm for 30 min and the precipitate was dispersed in 5 mL of deionized water. The PAH used here can prevent the aggregation of the Au@Ag NRs caused by 4MBA. The 4MBA tagged and PAH wrapped NPs were denoted as Au@Ag NR@4MBA@PAH.

2.2.3. Silica encapsulating of the SERS active Au@Ag NRs

The as-prepared Au@Ag NR@4MBA@PAH NPs were coated with an outer silica shell by a modified Stöber method [41]. 1 mL of 25 mg/mL PVP aqueous solution was added to 5 mL of the Au@Ag NR@4MBA@PAH solution and gently agitated for 15 h. The mixture was centrifuged once at 8000 rpm for 30 min and the precipitate was dispersed in 5 mL ethanol. Then 350 μL of ammonia water was added. The growth of the outer silica shell was initiated by 6 injections of 2 μL TEOS into the above mixture with an interval of 30 min. The reaction was further continued for 3 h. Finally the silica coated SERS active Au@Ag NRs (denoted as Au@Ag NR@4MBA@SiO_2) were collected by centrifugation at 7000 rpm for 20 min and washed repeatedly with ethanol and deionized water. The purified Au@Ag NR@4MBA@SiO_2 NPs were finally suspended in 5 mL of deionized water.

2.2.4. Conjugation of CdTe QDs and folic acid

3-mercaptopropionic acid (MPA) stabilized water soluble green luminescent CdTe QDs were synthesized as described elsewhere [42]. The cancer cell targeting probe was acquired by

covanlently adsorbing FA and CdTe QDs onto the surfaces of the Au@Ag NR@4MBA@SiO_2 NPs. 25 μL of 10% PEI aqueous solution was added to 5 mL of the as-synthesized Au@Ag NRs@4MBA@-SiO_2 solution and gently stirred for an hour. Afterwards, the excess PEI was removed by centrifugation thrice at 7000 rpm for 20 min. The pellet was suspended in 5 mL of PBS. 300 μL of CdTe QDs solution was added to 5 mL of PBS solution containing 1 mg FA under stirring. For the synthesis of the FA free probe (denoted as Au@Ag NR@4MBA@SiO_2@QDs), the CdTe QDs solution was added to the PBS solution without FA. Then 200 μL of 10 mM EDC (in PBS) and 40 μL of 0.1 M NHS aqueous solution were added to activate the carboxyl groups of FA as well as those of the MPA on CdTe QDs. 15 min later, 1 mL of the PEI functionalized NPs were added and the reaction was allowed to proceed for 12 h in the dark at room temperature. The excess CdTe QDs and FA were removed by centrifugation twice at 7000 rpm for 20 min. The pellet was dispersed in 1 mL of deionized water, yielding the cancer cell targeting probe (denoted as Au@Ag NRs@4MBA@SiO_2@QDs/FA).

2.3. Cell culture and in vitro experiments

HeLa cells and human embryonic lung fibroblasts (MRC-5) cells were purchased from China Type Culture Collection and cultured in medium (DMEM) under standard cell culture condition (5% CO_2, 37 °C). Media were supplemented with 10% fetal bovine serum (Biochrom) and 1% penicillin–streptomycin (Nanjing KeyGen Biotech. Co., Ltd.).

To examine the SERS and fluorescence performance of the targeting probe inside living cells, HeLa cells were seeded into culture dish (Corning) and incubated for 24 h. Then the targeting probe solution was added to the cell culture dish (volume ratio probe solution:culture media = 1:5). Three hours later, the culture media were discarded and the culture dish was gently washed with PBS before the SERS and fluorescence measurements.

To test the targeting capability of the cancer cell targeting probe, HeLa and MRC-5 cells were seeded into culture dishes and incubated for 24 h. Then the targeting probe solution and the FA free probe solution were added to the cell culture dishes (volume ratio probe solution:culture media = 1:5), respectively. An hour later, the culture media were discarded and the culture dishes were gently washed with PBS before the SERS and fluorescence measurements.

2.4. Instruments

Extinction spectra were measured by a Shimadzu UV-3600 PC spectrophotometer with quartz cuvettes of 1 cm path length. Photoluminescence emission spectra were measured by an Edinburg FLS920 spectrofluorimeter, the spectrum linewidth was 1.5 nm for the selected slit width at the excitation and emission of the spectrofluorimeter. Transmission electron microscope (TEM) images and energy dispersive X-ray (EDX) spectra were obtained with an FEI Tecnai G^2T20 electron microscope operating at 200 kV. SERS and fluorescence measurements were performed with a confocal microscope (FV 1000, Olympus). Fluorescent images of cells were recorded at 488 nm excitation and SERS spectra were obtained at

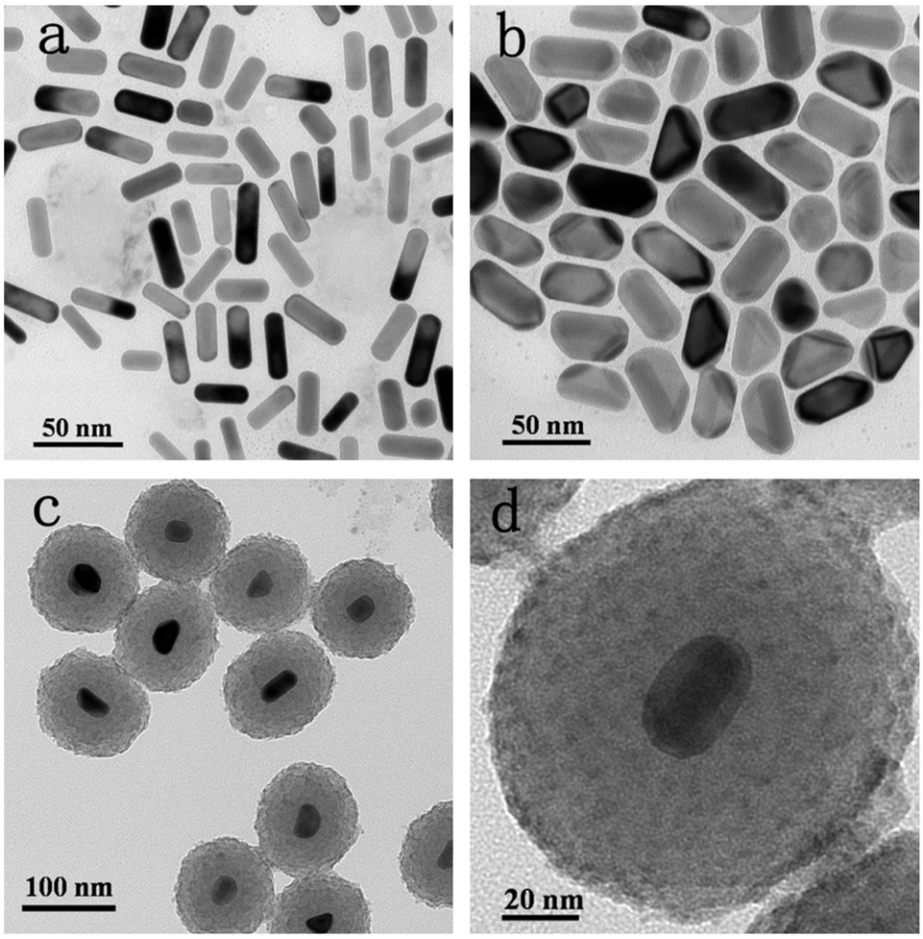

Fig. 1. TEM images of (a) GNRs, (b) Au@Ag NRs, (c) targeting probes, (d) enlarged TEM image of a single targeting probe.

633 nm excitation. The laser power was 2.3 mW at the sample position. Rayleigh scattering light was removed by a holographic notch filter. The Raman scattering light was directed to an Andor shamrock spectrograph equipped with a charge-coupled device (CCD).

3. Results and discussion

3.1. Characterization of the cancer cell targeting probe (denoted as Au@Ag NR@4MBA@SiO_2@QDs/FA)

To achieve silver NPs with a uniform size distribution to be used as the SERS substrates, the Au@Ag NRs were fabricated according to the strategy of Xiang et al. [36], which uses GNRs as the template for silver coating. The initial GNRs were synthesized through the seed-mediated growth method [40]. Comparing the TEM images of the GNRs and the Au@Ag NRs (shown in Fig. 1), the Au@Ag NRs seem to be fatter than GNRs, due to the coating of the silver shell. The average size of the GNRs is $(37\text{ nm}\pm3\text{ nm})\times(12\text{ nm}\pm2\text{ nm})$ while that of the Au@Ag NRs is $(46\text{ nm}\pm5\text{ nm})\times(24\text{ nm}\pm2\text{ nm})$. The epitaxial growth of the silver shell can also be confirmed by the extinction spectra (Fig. 2a). Upon the silver deposition, the longitudinal surface plasmon resonance (LSPR) band of GNRs peaked at 690 nm underwent a significant blue shift, whereas a new band arose at shorter wavelength around 400 nm. This result is consistent with that reported by Xiang et al. [36]. It has been shown that the LSPR band of the Au@Ag NRs can also be tuned from the visible to the near infrared region of the optical spectrum, similar to that of GNRs [32,36]. Thus, with corners and edges presented on their surfaces and the tunable optical properties, such silver coated core–shell nanorods can be employed as excellent candidates for SERS applications.

The as-prepared Au@Ag NRs are positively charged due to the surfactant molecules (CTAB) used in the synthesis process. After being tagged with the SERS reporter molecules (4MBA) through their thiol groups, the positive surface charge of the Au@Ag NRs will be disturbed, leading to the aggregation of the Au@Ag NRs. In our experiments, to avoid this aggregation, a layer of PAH is coated on the 4MBA-tagged Au@Ag NRs. As a result, monodisperse silica NPs were obtained with a single Au@Ag NR core inside each (shown in Fig. 1c). The extinction spectra in Fig. 2(a) also reveal that the Au@Ag NRs did not aggregate. The SPR band positions of the PAH wrapped 4MBA-tagged Au@Ag NRs (Au@Ag NR@4MBA@PAH) remained exactly the same to those of the Au@Ag NRs. Besides, no obvious tailing of the LSPR in the longer wavelength region was observed.

After the Au@Ag NR@4MBA@PAH NPs were prepared, an outer silica layer was achieved by a modified Stöber method [41].

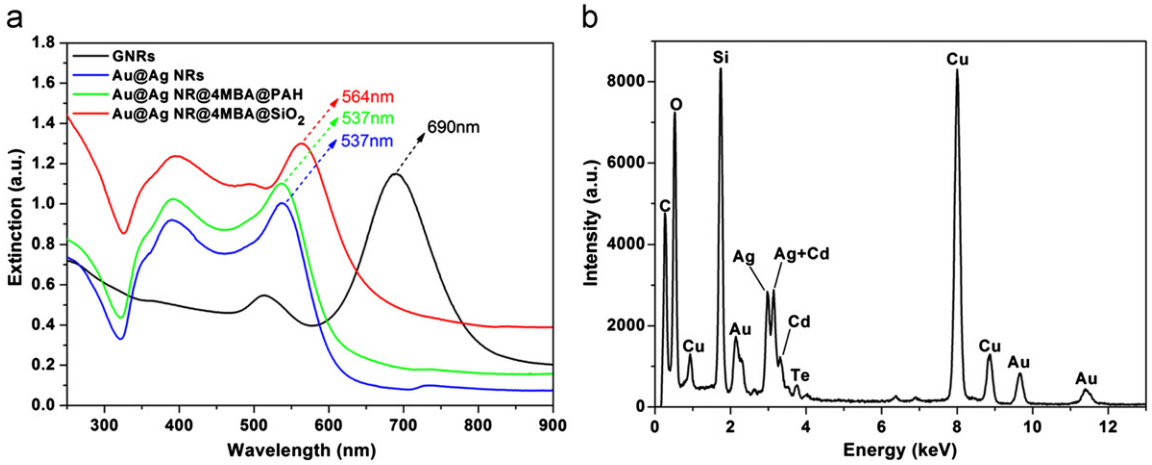

Fig. 2. (a) Extinction spectra obtained during the synthesis of the cancer cell targeting probe. (b) EDX spectrum of the cancer cell targeting probe. The Cu signal originates from the copper mesh.

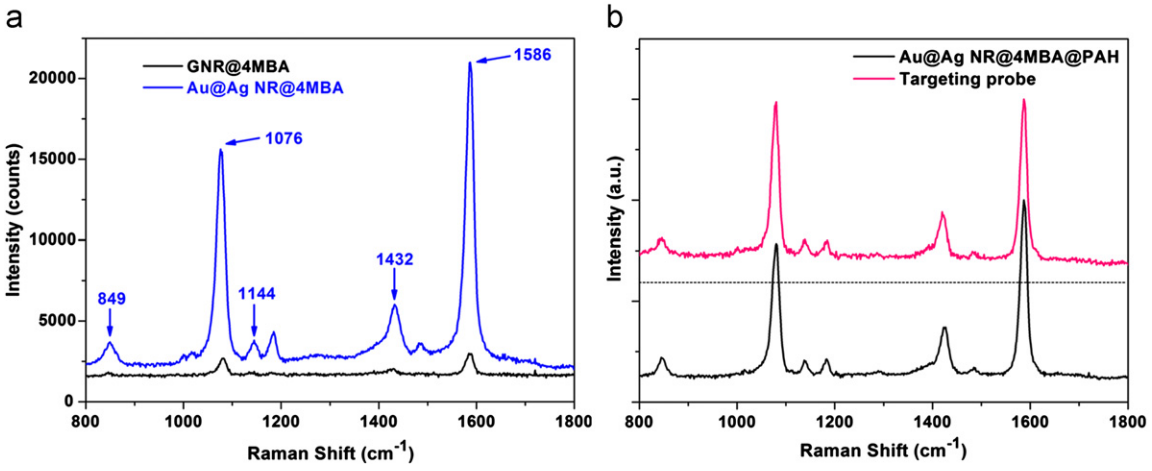

Fig. 3. (a) SERS signals obtained from 4MBA labeled GNRs and Au@Ag NRs; (b) SERS spectra of Au@Ag NR@4MBA@PAH and the targeting probe, the dashed line indicates the baseline of the SERS spectrum of the targeting probe. The spectra were placed in parallel for clarity. The integrating time of each SERS spectrum was 60 s.

For obtaining a more smooth silica shell, the Au@Ag NR@4MBA@-PAH NPs were first coated by the amphiphilic, nonionic polymer PVP and then transferred to a mixed solution of ammonia and ethanol. After the injection of a proper amount of TEOS, a homogeneous silica shell with a thickness of ~40 nm was formed. As shown in Fig. 2(a), the silica coating process only induced red shift of the whole extinction spectrum of the NPs due to the increase in the refractive index, while no further tailing of the LSPR band was observed. This result corresponds well with the fact that only a single Au@Ag NR was encapsulated in each silica nanoparticle. Finally, after modifying the surfaces of the Au@Ag NR@4MBA@SiO_2 NPs with amino groups by PEI, FA and CdTe QDs were conjugated to the silica shell using EDC and NHS as the zero length cross-linkers. Thus the cell targeting probe (denoted as Au@Ag NR@4MBA@SiO_2@QDs/FA) was obtained, whose TEM images were shown in Fig. 1(c and d). The average diameter of the final probe is 115 nm ± 6 nm. It can be observed from Fig. 1(d) that the targeting probe has a roughened surface, which indicates the successful attachment of CdTe QDs. Besides, the EDX spectrum of the targeting probe clearly demonstrates the signals of Au, Ag, Si, Cd and Te (shown in Fig. 2b), which also proves that the fabricated probe exhibits a structure as expected.

3.2. SERS and fluorescence performance of the targeting probe

The Au@Ag NRs are chosen as the SERS substrates because they possess not only a superior SERS enhancing capability but also a well monodisperse morphology [35]. Fig. 3(a) shows the measured SERS signals from 4MBA-labeled GNRs and Au@Ag NRs under the same experimental conditions. The SERS spectrum of 4MBA has been well assigned previously [43]. The two dominant peaks at 1076 cm^{-1} and 1586 cm^{-1} are assigned to the ring-breathing modes. The Raman band at 849 cm^{-1} is attributed to the COO^- bending mode ($\delta(COO^-)$) and that at 1144 cm^{-1} is attributed to a mixed mode ($13\beta(CCC)+\nu(C–S)+\nu(C–COOH)$). Besides, the one at 1432 cm^{-1} is ascribed to the $\nu_s(COO^-)$ stretching mode. Comparing the two spectra in Fig. 3(a), it is obvious that the Au@Ag NRs can generate much stronger SERS signals than the GNRs, resulting in an increased SERS activity as expected.

The influence of the silica coating, QDs and FA conjugation over the SERS performance of the targeting probe was carefully investigated, using the excitation wavelength of 633 nm. As shown in Fig. 3(b), the intense and robust SERS signal of the probe was well maintained through both the silica coating and the surface modification procedures. Moreover, no fluorescence background from CdTe QDs was observed.

In the structure of our presented targeting probe, the FA molecules and CdTe QDs were both anchored to the outmost silica surfaces. Here, FA serves as the targeting ligand while CdTe acts as the fluorescent contrast agent. In the experiments, amino groups were first introduced onto the surfaces of the Au@Ag NR@4MBA@SiO_2 NPs by the electrostatic adsorption of branched PEI molecules. PEI functionalized NPs have a much higher surface concentration of amino groups compared to those prepared by classical co-condensation using amino silanes [2,44]. Then the CdTe QDs and FA were covalently conjugated to the amino groups via standard carboxyl-amine conjugation chemistry using EDC and NHS as the coupling agents [2]. As is well known, the fluorescence of QDs or organic dyes will be quenched upon the direct contact with a metal surface due to the nonradiative energy transfer from the fluorophores to the metal. However, in our probe, the silica shell can virtually prevent the occurrence of quenching. The photoluminescence spectrum of the targeting probe is shown in Fig. 4, using an excitation wavelength of 400 nm. Obviously, the fluorescence of CdTe QDs was well kept and no SERS signals were observed. When illuminated by the UV-light, the targeting probe was able to generate bright green light (see the inset of Fig. 4). All the above experimental results demonstrate that the multifunctional cancer cell targeting probe can generate both SERS and fluorescence signals, which can be switched by using different excitation wavelengths. The strong SERS signals supported by the Au@Ag NRs and fluorescence signals generated by QDs reveal that the proposed targeting probes possess a superior sensitivity during the cancer cell targeting process. Besides, more than 30 batches of the targeting probes have been synthesized, which all presented excellent

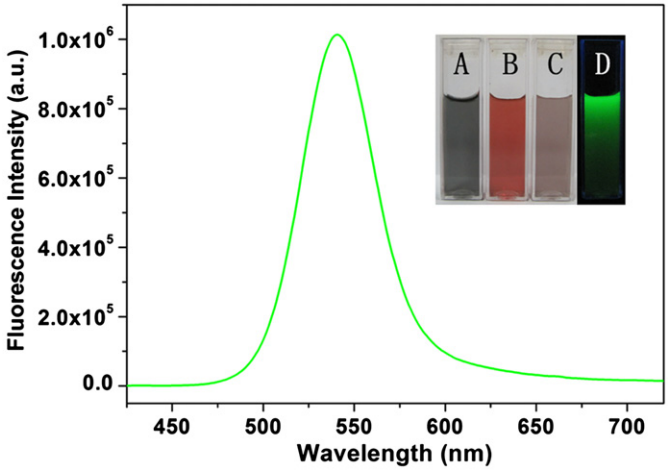

Fig. 4. Photoluminescence spectra of the targeting probe excited at 400 nm. Inset shows the digital photograph of the (A) GNRs, (B) Au@Ag NRs, (C) targeting probes, (D) targeting probes illuminated by 365 nm UV-light.

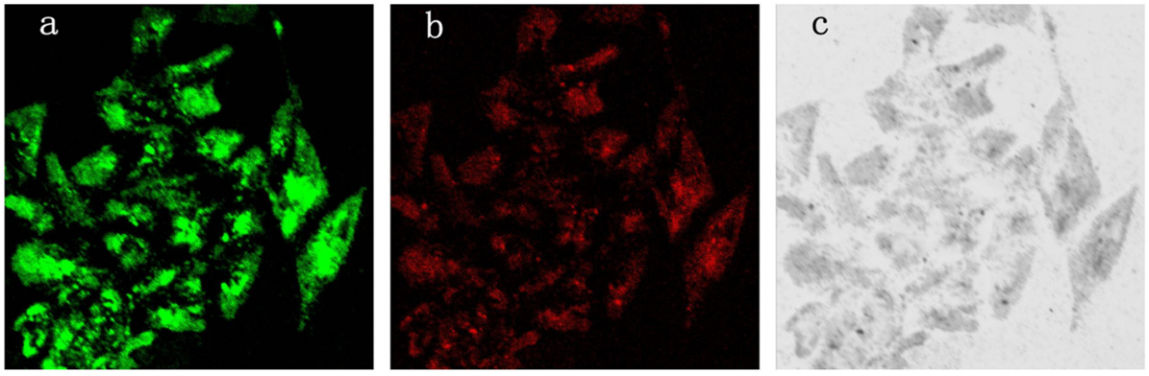

Fig. 5. (a) Fluorescence imaging, (b) SERS mapping and (c) bright field imaging of HeLa cells incubated with the targeting probes for 3 h. The excitation wavelength of the fluorescence imaging was 488 nm while that of the SERS mapping was 633 nm.

SERS and fluorescence properties with a uniform morphology, indicating the well reproducibility of the targeting probes.

3.3. In vitro experiments

To evaluate the performance of the proposed probe inside living cells, HeLa cells were incubated with the targeting probes for 3 h to allow a sufficient cellular uptake of the probe. Then the targeting probe loaded HeLa cells were subjected to the fluorescence and SERS imaging. The results are shown in Fig. 5. According to Fig. 5(c), the probes incorporated by HeLa cells can clearly be observed as the black dots. When excited at 488 nm, strong fluorescence was obtained from these HeLa cells (Fig. 5a). However, no obvious fluorescence was observed from the HeLa cells without the probes inside, indicating that the strong fluorescence was not the cellular auto fluorescence. Then, SERS mapping of the same HeLa cells was also acquired by changing the excitation wavelength to 633 nm (Fig. 5b). The SERS signal of 4MBA was well preserved and no fluorescence background was detected, as shown in Fig. 6. The results indicate that the proposed probe is capable of keeping their distinct SERS and fluorescence performances after being taken up by living cells.

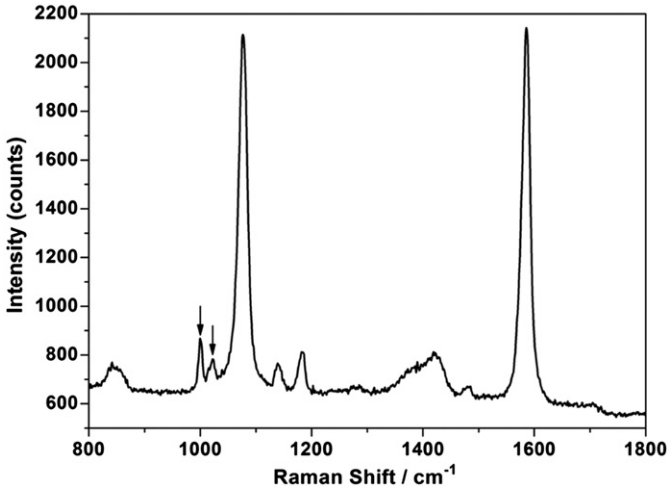

Fig. 6. SERS spectrum acquired from the targeting probe loaded HeLa cells. The excitation wavelength was 633 nm with an integrating time of 60 s. The Raman peaks pointed by the arrows belong to the bottom of the culture dish.

It was reported that when the FA decorated NPs are subjected to cells overexpressing folate receptors (FRs), the cellular uptake of the NPs can be greatly improved by the FRs mediated endocytosis [45,46]. Thus, HeLa cells which overexpress FRs on their membranes [47] were chosen as the model target cancer cells to examine the targeting ability of the presented probe. FA free probes and folate receptor negative MRC-5 cells were chosen as the negative controls. After being incubated with the corresponding probes, the cells were subjected to fluorescence imaging and SERS mapping. As shown in Fig. 7, HeLa cells incubated with the targeting probes (Fig. 7a–d) generated much stronger fluorescence and SERS signals than HeLa cells incubated with the FA free control probes (Fig. 7e–h) and MRC-5 cells incubated with the targeting probes (Fig. 7i–l). This indicates that more targeting probes were

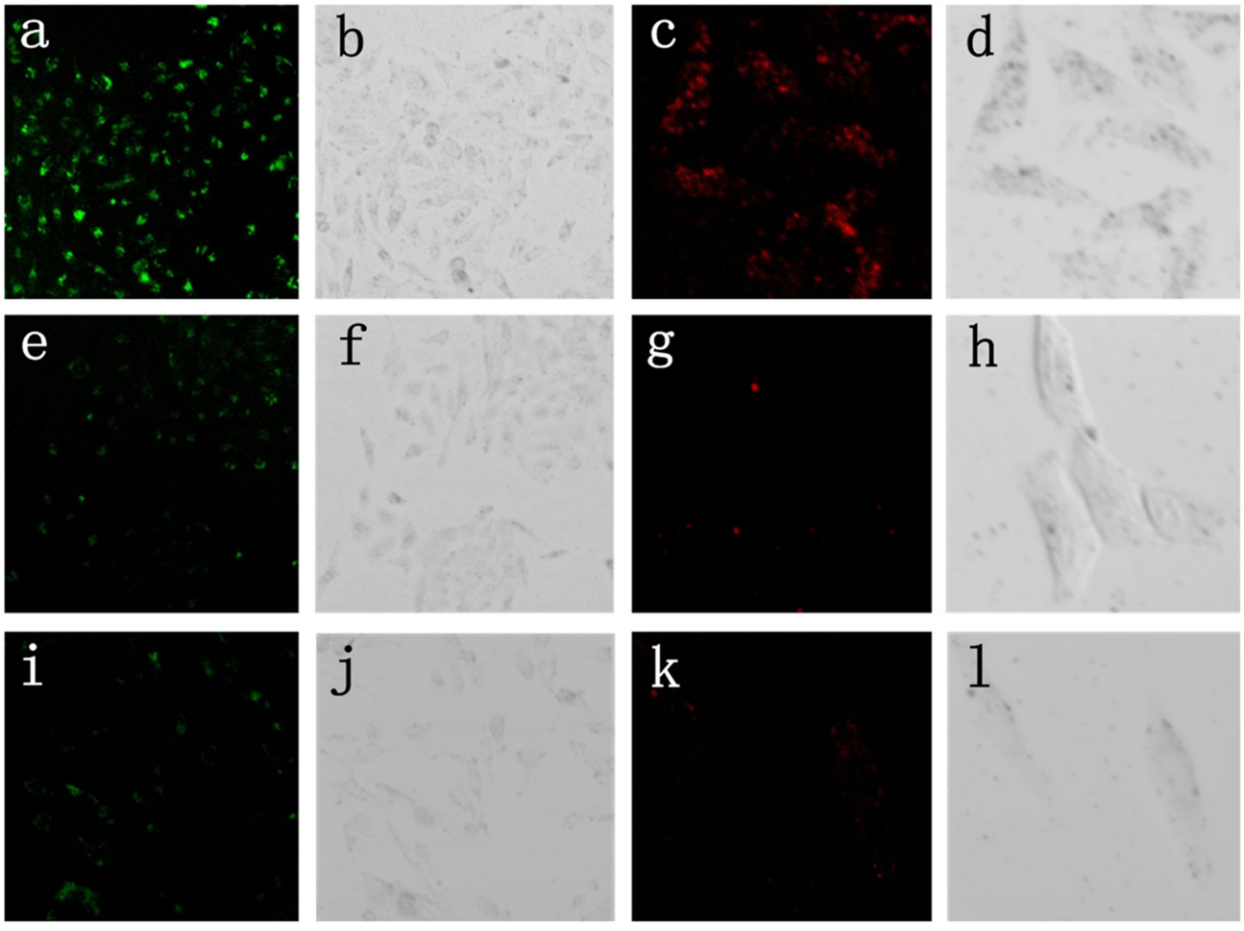

Fig. 7. (a, b) Fluorescence image and (c, d) SERS mapping of HeLa cells incubated with the targeting probe; (e, f) fluorescence image and (g, h) SERS mapping of HeLa cells incubated with FA free probe; (i, j) fluorescence image and (k, l) SERS mapping of MRC-5 cells incubated with the targeting probe.

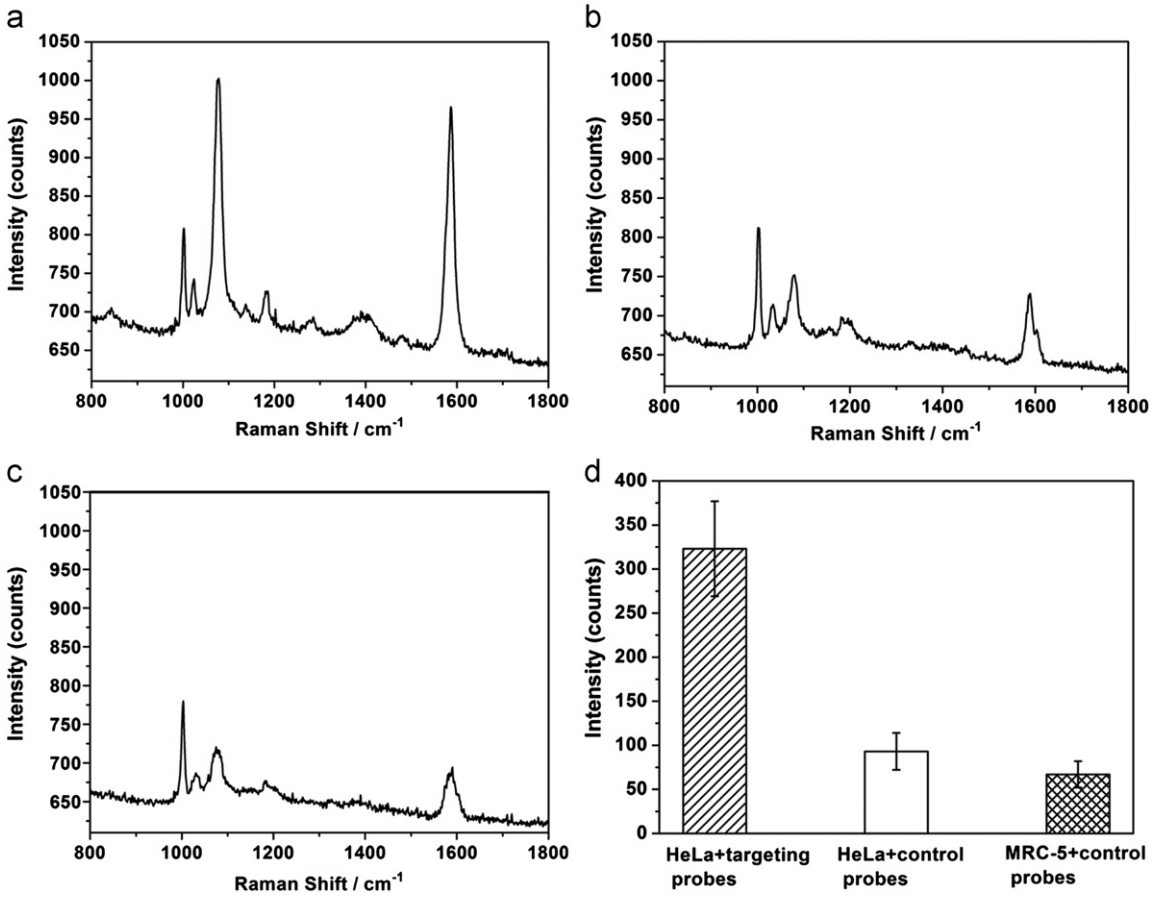

Fig. 8. (a) SERS spectrum obtained from HeLa cells incubated with the targeting probe; (b) SERS spectrum obtained from HeLa cells incubated with the FA free probe; (c) SERS spectrum obtained from MRC-5 cells incubated with the targeting probe; for each situation, the SERS spectra were collected from 10 randomly selected cells and average results were presented. (d) Intensity of the 1076 cm^{-1} peak. The error bars represent the standard deviation of 10 measurements.

taken up by the FRs overexpressed HeLa cells. Thus, both the fluorescence imaging and the SERS mapping results revealed the increased cellular uptake of the targeting probe compared with that of the two negative controls. These results indicate that the overexpression of FRs on HeLa cells may facilitate the recognition of FA conjugated NPs and increase the cellular uptake through the FRs mediated endocytosis. The SERS spectra obtained during the *in vitro* comparison experiments were shown in Fig. 8. Fig. 8(a) shows the SERS spectrum acquired from HeLa cells incubated with the targeting probes and Fig. 8(b) demonstrates the SERS spectrum acquired from HeLa cells incubated with the FA free control probes, while Fig. 8(c) exhibits the SERS spectrum obtained from MRC-5 cells incubated with the targeting probes. HeLa cells incubated with the targeting probes obviously provided the strongest SERS signals. As shown in Fig. 8(d), SERS signals measured from HeLa cells incubated with the targeting probes are about 3 times higher than those from the two controls. These results showed that the proposed targeting probe can recognize FRs overexpressed cancer cells with a high selectivity and greatly improve the cellular uptake of the targeting probe through the FRs mediated endocytosis.

4. Conclusions

We have demonstrated the successful fabrication of a SERS and fluorescence dual mode cancer cell targeting probe based on silica coated Au@Ag NRs conjugated with CdTe QDs and FA. The targeting probe has the intense SERS signals under the light excitation at wavelength of 633 nm without the fluorescence background. It also provides a highly bright and stable fluorescence for cell imaging when the excitation wavelength is switched to 488 nm. The special SERS and fluorescence performance of the probe was well preserved after being taken up by living cells. Finally, the HeLa cells with overexpressed FRs were specifically targeted by the presented probe. With the targeting and multiplex imaging abilities, this kind of multifunctional probe has unique potential for tracking the nanoparticle-based systems containing multiple components (such as drug delivery systems), where the different components (such as drugs and nanocarriers) can be monitored through fluorescence or SERS, respectively. Other potential applications of this kind of multifunctional probe include optical coding, highly sensitive biosensing and so on. Further experiments are being conducted to explore those applications.

Acknowledgment

This work was supported by Natural Science Foundation of China (NSFC) (nos. 60708024, 60877024, 61177033, and 21104009), the Specialized Research Fund for the Doctoral Program of Higher Education (SRFDP) (nos. 20070286058 and 20090092110015), Science Foundation for The Excellent Youth Scholars of Southeast University, and the Scientific Research Foundation of Graduate School of Southeast University (YBJJ1125).

References

[1] K. Riehemann, S.W. Schneider, T.A. Luger, B. Godin, M. Ferrari, H. Fuchs, Angew. Chem. Int. Ed. 48 (2009) 872–897.

[2] J.M. Rosenholm, A. Meinander, E. Peuhu, R. Niemi, J.E. Eriksson, C. Sahlgren, M. Linden, ACS Nano 3 (2009) 197–206.
[3] L. Tong, Y. Zhao, T.B. Huff, M.N. Hansen, A. Wei, J.-X. Cheng, Adv. Mater. 19 (2007) 3136–3141.
[4] C. Zavaleta, A. de la Zerda, Z. Liu, S. Keren, Z. Cheng, M. Schipper, X. Chen, H. Dai, S.S. Gambhir, Nano Lett. 8 (2008) 2800–2805.
[5] H. He, Y. Li, X.-R. Jia, J. Du, X. Ying, W.-L. Lu, J.-N. Lou, Y. Wei, Biomaterials 32 (2011) 478–487.
[6] M. Liong, J. Lu, M. Kovochich, T. Xia, S.G. Ruehm, A.E. Nel, F. Tamanoi, J.I. Zink, ACS Nano 2 (2008) 889–896.
[7] E.-Q. Song, J. Hu, C.-Y. Wen, Z.-Q. Tian, X. Yu, Z.-L. Zhang, Y.-B. Shi, D.-W. Pang, ACS Nano 5 (2011) 761–770.
[8] Z. Wang, S. Zong, J. Yang, J. Li, Y. Cui, Biosens. Bioelectron. 26 (2011) 2883–2889.
[9] W. Xia, P.S. Low, J. Med. Chem. 53 (2010) 6811–6824.
[10] M. Das, D. Mishra, P. Dhak, S. Gupta, T.K. Maiti, A. Basak, P. Pramanik, Small 5 (2009) 2883–2893.
[11] J.-M. Oh, S.-J. Choi, G.-E. Lee, S.-H. Han, J.-H. Choy, Adv. Funct. Mater. 19 (2009) 1617–1624.
[12] H.-S. Cho, Z. Dong, G.M. Pauletti, J. Zhang, H. Xu, H. Gu, L. Wang, R.C. Ewing, C. Huth, F. Wang, D. Shi, ACS Nano 4 (2010) 5398–5404.
[13] R. Di Corato, N.C. Bigall, A. Ragusa, D. Dorfs, A. Genovese, R. Marotta, L. Manna, T. Pellegrino, ACS Nano 5 (2011) 1109–1121.
[14] C.-H. Lee, S.-H. Cheng, Y. Wang, Y.-C. Chen, N.-T. Chen, J. Souris, C.-T. Chen, C.-Y. Mou, C.-S. Yang, L.-W. Lo, Adv. Funct. Mater. 19 (2009) 215–222.
[15] S.H. Nam, Y.M. Bae, Y.I. Park, J.H. Kim, H.M. Kim, J.S. Choi, K.T. Lee, T. Hyeon, Y.D. Suh, Angew. Chem. Int. Ed. 50 (2011) 6093–6097.
[16] X.H. Gao, Y.Y. Cui, R.M. Levenson, L.W.K. Chung, S.M. Nie, Nat. Biotechnol. 22 (2004) 969–976.
[17] X. Michalet, F.F. Pinaud, L.A. Bentolila, J.M. Tsay, S. Doose, J.J. Li, G. Sundaresan, A.M. Wu, S.S. Gambhir, S. Weiss, Science 307 (2005) 538–544.
[18] M. Bruchez, M. Moronne, P. Gin, S. Weiss, A.P. Alivisatos, Science 281 (1998) 2013–2016.
[19] W.C.W. Chan, S.M. Nie, Science 281 (1998) 2016–2018.
[20] H. Park, S. Lee, L. Chen, E.K. Lee, S.Y. Shin, Y.H. Lee, S.W. Son, C.H. Oh, J.M. Song, S.H. Kang, J. Choo, Phys. Chem. Chem. Phys. 11 (2009) 7444–7449.
[21] C. Song, Z. Wang, R. Zhang, J. Yang, X. Tan, Y. Cui, Biosens. Bioelectron. 25 (2009) 826–831.
[22] G. von Maltzahn, A. Centrone, J.-H. Park, R. Ramanathan, M.J. Sailor, T.A. Hatton, S.N. Bhatia, Adv. Mater. 21 (2009) 3175–3180.
[23] S. Zong, Z. Wang, J. Yang, Y. Cui, Anal. Chem. 83 (2011) 4178–4183.
[24] K. Kneipp, Y. Wang, H. Kneipp, L.T. Perelman, I. Itzkan, R. Dasari, M.S. Feld, Phys. Rev. Lett. 78 (1997) 1667–1670.
[25] S.M. Nie, S.R. Emery, Science 275 (1997) 1102–1106.
[26] Y. Wang, J.L. Seebald, D.P. Szeto, J. Irudayaraj, ACS Nano 4 (2010) 4039–4053.
[27] J. Chen, J.M. McLellan, A. Siekkinen, Y. Xiong, Z.-Y. Li, Y. Xia, J. Am. Chem. Soc. 128 (2006) 14776–14777.
[28] C.J. Orendorff, L. Gearheart, N.R. Jana, C.J. Murphy, Phys. Chem. Chem. Phys. 8 (2006) 165–170.
[29] Z. Wang, S. Zong, J. Yang, C. Song, J. Li, Y. Cui, Biosens. Bioelectron. 26 (2010) 241–247.
[30] J.-H. Kim, W.W. Bryan, T.R. Lee, Langmuir 24 (2008) 11147–11152.
[31] M. Sanles-Sobrido, W. Exner, L. Rodriguez-Lorenzo, B. Rodriguez-Gonzalez, M.A. Correa-Duarte, R.A. Alvarez-Puebla, L.M. Liz-Marzan, J. Am. Chem. Soc. 131 (2009) 2699–2705.
[32] M.Z. Liu, P. Guyot-Sionnest, J. Phys. Chem. B 108 (2004) 5882–5888.
[33] Y. Khalavka, J. Becker, C. Soennichsen, J. Am. Chem. Soc. 131 (2009) 1871–1875.
[34] J.H. Song, F. Kim, D. Kim, P.D. Yang, Chem. Eur. J. 11 (2005) 910–916.
[35] M.F. Cardinal, B. Rodriguez-Gonzalez, R.A. Alvarez-Puebla, J. Perez-Juste, L.M. Liz-Marzan, J. Phys. Chem. C 114 (2010) 10417–10423.
[36] Y. Xiang, X. Wu, D. Liu, Z. Li, W. Chu, L. Feng, K. Zhang, W. Zhou, S. Xie, Langmuir 24 (2008) 3465–3470.
[37] Y. Cui, X.-S. Zheng, B. Ren, R. Wang, J. Zhang, N.-S. Xia, Z.-Q. Tian, Chem. Sci. 2 (2011) 1463–1469.
[38] S. Lee, H. Chon, S.-Y. Yoon, E.K. Lee, S.-I. Chang, D.W. Lim, J. Choo, Nanoscale 4 (2012) 124–129.
[39] Z. Wang, S. Zong, H. Chen, H. Wu, Y. Cui, Talanta 86 (2011) 170–177.
[40] I. Gorelikov, N. Matsuura, Nano Lett. 8 (2008) 369–373.
[41] C. Graf, D.L.J. Vossen, A. Imhof, A. van Blaaderen, Langmuir 19 (2003) 6693–6700.
[42] C. Wang, M. Fang, J. Han, H. Zhang, Y. Cui, B. Yang, J. Phys. Chem. C 113 (2009) 19445–19451.
[43] C.E. Talley, L. Jusinski, C.W. Hollars, S.M. Lane, T. Huser, Anal. Chem. 76 (2004) 7064–7068.
[44] J.M. Rosenholm, M. Linden, Chem. Mater. 19 (2007) 5023–5034.
[45] R.J. Lee, P.S. Low, J. Biol. Chem. 269 (1994) 3198–3204.
[46] K.S. Soppimath, L.-H. Liu, W.Y. Seow, S.-Q. Liu, R. Powell, P. Chan, Y.Y. Yang, Adv. Funct. Mater. 17 (2007) 355–362.
[47] S.Y. Chan, C.J. Empig, F.J. Welte, R.F. Speck, A. Schmaljohn, J.F. Kreisberg, M.A. Goldsmith, Cell 106 (2001) 117–126.